Tumor and Stem Cell Biology

Cancer Research

Cell-Cycle Regulation Accounts for Variability in Ki-67 Expression Levels

Michal Sobecki[1], Karim Mrouj[1], Jacques Colinge[2], François Gerbe[3], Philippe Jay[3], Liliana Krasinska[1], Vjekoslav Dulic[1], and Daniel Fisher[1]

Abstract

The cell proliferation antigen Ki-67 is widely used in cancer histopathology, but estimations of Ki-67 expression levels are inconsistent and understanding of its regulation is limited. Here we show that cell-cycle regulation underlies variable Ki-67 expression in all situations analyzed, including nontransformed human cells, normal mouse intestinal epithelia and adenomas, human cancer cell lines with or without drug treatments, and human breast and colon cancers. In normal cells, Ki-67 was a late marker of cell-cycle entry; Ki-67 mRNA oscillated with highest levels in G_2 while protein levels increased throughout the cell cycle, peaking in mitosis. Inhibition of CDK4/CDK6 revealed proteasome-mediated Ki-67 degradation in G_1. After cell-cycle exit, low-level Ki-67 expression persisted but was undetectable in fully quiescent differentiated cells or senescent cells. CDK4/CDK6 inhibition *in vitro* and in tumors in mice caused G_1 cell-cycle arrest and eliminated Ki-67 mRNA in RB1-positive cells but had no effect in RB1-negative cells, which continued to proliferate and express Ki-67. Thus, Ki-67 expression varies due to cell-cycle regulation, but it remains a reliable readout for effects of CDK4/CDK6 inhibitors on cell proliferation. *Cancer Res; 77(10); 2722–34. ©2017 AACR.*

Introduction

Ki-67 is a nuclear protein expressed in all proliferating vertebrate cells, and it is a widely used biomarker to estimate the proportion of dividing cells to grade tumors. Ki-67 expression might have prognostic value, such as in the IHC4+C score in breast cancer (1). However, inconsistency in assessments of Ki-67 labeling index hinders its use to stratify patients for therapy (2). This variability might contribute to inconsistency regarding the prognostic value of Ki-67 labeling index in a given cancer type, for example, triple-negative breast cancer (TNBC; refs. 3, 4). Therefore, it is critical to define what constitutes Ki-67–positive expression and what the clinical significance of different Ki-67 levels is. This requires a better understanding of the control and functional significance of Ki-67 expression.

In cultured cells, Ki-67 levels are highest in G_2 phase and mitosis (5). In HL60 cells, Ki-67 protein was reported highly unstable throughout the cell cycle (6), but this has not been confirmed in other cell lines. Furthermore, Ki-67 transcriptional control is poorly understood. The *MKI67* promoter of the gene encoding Ki-67 is GC-rich, contains Sp1-binding sites, but lacks a TATA box (7, 8). In primary fibroblasts, it is bound by E2F proteins (9), and Ki-67 mRNA accumulates upon E2F overexpression (10). E2F-dependent transcription, which is required for S-phase onset, is repressed by RB family proteins, whose phosphorylation by cyclin-dependent kinases (CDK) promotes cell-cycle progression. Although RB expression is lost in many cancers, it is not clear whether this leads to upregulation of Ki-67. It is also not known whether Ki-67 is frequently over- or underexpressed in cancers, for example, due to copy number variation, translational regulation, or mutation of sites affecting protein stability or promoter activity.

We, and others, recently showed that Ki-67 is not required for proliferation of mammalian cells in culture (11–13). Furthermore, mice with a disrupted *Mki67* gene were healthy and fertile, despite minimal Ki-67 expression (11). Conversely, mice lacking the *Fzr1* gene maintained Ki-67 in differentiated, nonproliferating tissues (11). Thus, Ki-67 expression can be uncoupled from, and is not required for, cell proliferation. This raises the possibility that Ki-67 staining in cancers might not always reflect cell proliferation.

Like Ki-67, CDK4 and CDK6, which trigger RB phosphorylation, are not essential for cell proliferation in most cell types in mice (14). Nevertheless, CDK4 and D-type cyclins are required for certain cancers, including breast cancers (15). CDK4/CDK6 inhibition with PD0332991 (palbociclib) has shown major benefits in breast cancer clinical trials, leading to its approval in certain clinical settings (16), and it is currently in trials for a variety of other cancers. Preclinical models using tumor explants suggest that RB-positivity can predict responses to palbociclib (17). However, in these

[1]IGMM, CNRS Univ. Montpellier, Montpellier, France. [2]IRCM, INSERM ICM, Univ. Montpellier, Montpellier, France. [3]IGF, CNRS, INSERM, Univ. Montpellier, Montpellier, France.

Note: Supplementary data for this article are available at Cancer Research Online (http://cancerres.aacrjournals.org/).

M. Sobecki and K. Mrouj contributed equally to this article.

Current address for M. Sobecki: Department of Genome Biology, Institute for Integrative Biology of the Cell (I2BC), UMR 9198, CEA/CNRS/Université Paris Sud, Gif-sur-Yvette, Paris 91190, France.

Corresponding Author: Daniel Fisher, Institute of Molecular Genetics of Montpellier, CNRS, 1919 Route de Mende, Montpellier 34293, France. Phone/Fax: 334-3435-9694; E-mail: daniel.fisher@igmm.cnrs.fr

doi: 10.1158/0008-5472.CAN-16-0707

AACR

experiments, palbociclib effects were determined by Ki-67 expression itself. Yet Ki-67 expression may be directly promoted by CDK4/CDK6–dependent RB phosphorylation. Thus, upon CDK4/CDK6 inhibition, it remains possible that cells might continue to proliferate without Ki-67 expression. It is therefore essential to determine whether loss of Ki-67 after CDK4/CDK6 inhibition indeed reflects cell-cycle arrest by correlating with independent markers of cell proliferation.

In this study, we show that variability of Ki-67 levels is due to cell-cycle regulation of Ki-67 mRNA and protein in normal human cells, proliferating tissues in mice and human cancers. Furthermore, in cells that have recently exited the cell cycle, low-level Ki-67 persists. Ki-67 protein is degraded from mitosis to G_1, and G_1 arrest by CDK4/CDK6 inhibition causes loss of Ki-67 mRNA. Effects of palbociclib on Ki-67 expression always correlated with its effects on cell proliferation, including *in vivo*. These results have important implications for interpreting Ki-67 staining in cancer histopathology and for its use as a diagnostic marker.

Materials and Methods

Ethics

All animal experiments were performed in accordance with international ethics standards and were subjected to approval by the Animal Experimentation Ethics Committee of Languedoc Roussillon.

Mouse lines

The *Apc*^{lox} (*Apc*$^{tm2.1Cip}$) line (18) was provided by C. Perret (Cochin Institute, Paris, France). The *Villin-Cre*^{ERT2} line (19) was provided by S. Robine (Curie Institute, Paris, France).

Cell lines

Cell lines were not authenticated but were mycoplasma-free (tested weekly using Mycoalert kit). Normal human diploid foreskin fibroblasts (HDF) were from frozen stocks provided by J. Piette (CRBM, Montpellier, France) in 2001. IMR-90, U2OS, HeLa, HCT-116, MCF7, MDA-MB-231, MDA-MB-468, CAL51, HBL100, and IMR90 were originally obtained from the ATCC from 2000 to 2010. IMR-90 fibroblasts expressing HPV-16 E7 oncogene were described previously (20). U2OS, HeLa HCT-116, MCF7, MDA-MB-231, CAL51, and HBL100 were grown in DMEM with 10% FBS. HDFs were grown in DMEM supplemented with 10% FCS and 2 mmol/L L-glutamine. Cells were grown under standard conditions at 37°C in a humidified incubator containing 5% CO2. IMR-90 WT and E7 were grown in 3% oxygen in DMEM/F12 medium supplemented with 10% FBS and 4 mmol/L L-glutamine.

Cell drug treatments

Primary cells (HDF, BJ hTERT, IMR90) were treated with 1 μmol/L PD0332991 (Tocris), 100 μg/mL cycloheximide, 20 μmol/L MG132 (Tocris), 10 μg/mL bleomycin (Sigma-Aldrich), or 2 μg/mL ICRF-193 (Sigma-Aldrich).

Cell synchronization

G_0 block. HDF at 20% confluency were washed with PBS and incubated with medium supplemented with 0.1% FBS for 72 hours. Cell-cycle entry was stimulated by adding fresh medium with 10% FBS. Onset of S-phase was observed 16 hours later by EdU incorporation.

G_1–S block. HDF at 25% confluency were incubated with medium supplemented with 2 mmol/L thymidine or 2 mmol/L hydroxyurea for 24 hours. Cells were released from G_1–S block by washing twice with fresh medium for 5 minutes.

G_2 block. Seven hours after release from G_1–S block, HDFs were incubated with 9 μmol/L RO3306 (Tocris) for 14 hours. Cells were released from G_2 block by washing twice with fresh medium for 5 minutes. Mitosis was observed around 1 hour after release.

Cell extracts and gel electrophoresis

Frozen washed cell pellets were lyzed directly in Laemmli buffer at 95°C (without β-mercaptoethanol and bromophenol blue) and sonicated on ice for 10 minutes in 30 seconds/30 seconds ON/OFF intervals. Protein concentrations were determined by BCA assay. Proteins were separated by SDS-PAGE (7.5% and 12.5% gels) at 35 mA in TGS buffer and transferred to Immobilon membranes with a semidry blotting apparatus.

Dot blot

Ten micrograms of total cell lysate in 5 μL was spotted onto nitrocellulose, blocked, and probed using standard immunoblotting procedues. Signals were quantified using PXi4 Imaging System (Syngene) and GeneTools analysis software.

Antibodies

Antibodies were: Ki-67: clone SP6 (Abcam), 35 (BD Biosciences), SolA15 (eBioscience); RB1 (BD Biosciences); cyclin A: 6E6 (Novocastra), H-432 (Santa Cruz Technology); cyclin E1: HE12 (Santa Cruz Biotechnology); cyclin D1: DSC6 (Cell Signaling Technology), EP272Y (Millipore); cyclin B1: GNS1 (Santa Cruz Biotechnology); CNDKN1A: C-19 (Santa Cruz Biotechnology); phospho-histone H3S10: 9701 (Cell Signaling Technology).

qRT-PCR

Purified RNA (1,000 ng) extracted by RNeasy Mini Kit (Qiagen) was reverse-transcribed using SuperScript II Reverse Transcriptase (Life Technologies) according to the manufacturer's instructions. qPCR was performed using LightCycler 480 SYBR Green I Master (Roche) and LightCycler 480 qPCR machine with conditions: 95°C 10 minutes, 40 cycles of 95°C 20 seconds, 58°C 20 seconds, and 72°C 20 seconds. Reaction specificity was verified by melt curve analysis. Each sample was performed in three replicates. qPCR primers used were:

MKI67 (F: TGACCCTGATGAGAAAGCTCAA, R: CCCTGAGCAACACTGTCTTTT);

CCNA2 (F: AGGAAAACTTCAGCTTGTGGG, R: CACAAACTCTGCTACTTCTGGG);

CCNE1 (F: CCGGTATATGGCGACACAAG, R: ACATACGCAAACTGGTGCAA);

PCNA (F: CCTGCTGGGATATTAGCTCCA, R: CAGCGGTAGGTGTCGAAGC);

CCNB1 (F: TGTGTCAGGCTTTCTCTGATG, R: TTGGTCTGACTGCTTGCTCT);

CCND1, (F: GCTGCGAAGTGGAAACCATC, R: CCTCCTTCTG-CACACATTTGAA);

B2M (F: GCGCTACTCTCTCTTTCTGG, R: AGAAAGACCAG-TCCTTGCTGA);

RPL19 (F: ATGCCGGAAAAACACCTTGG, R: GTGACCTTCT-CTGGCATTCG).

Proliferation and senescence assays

Analysis of DNA replication in cells was achieved by treatment with 2 mmol/L 5-ethynyl-2'-deoxyuridine (EdU; Life Technologies) before fixation. Replicating cells were visualized following the protocol from Click-iT EdU AlexaFluor-488 Imaging Kit (Life Technologies). Beta-galactosidase staining was conducted using Senescence Detection Kit (ab65351) following the manufacturer's instructions.

Xenografts

Three million log-phase viable mouse pathogen-free (IMPACT1, Iddex) MDA-MB-231 and MDA-MB-468 cells in 0.2 mL, 50% v/v Matrigel (BD Biosciences) were injected subcutaneously into 6-week-old female athymic nu/nu mice (Envigo). Tumors were grown to an average volume of 150–200 mm^3 measured by caliper using the formula "$\pi/6 \times S^2$ (smaller radius) $\times$ L (larger radius)" before initiation of treatment. Mice were then randomized into treatment groups for each cell line: vehicle control or 150 mg/kg/day PD 0332991. PD 0332991 was orally administered (gavage) as a solution in 50 mmol/L sodium lactate, pH 4 for 5 consecutive days. Following this treatment, mice were euthanized by cervical dislocation, and tumors were excised by dissection. For each tumor sample, one part was fixed in 10% formalin overnight before transfer into 70% ethanol and another snap frozen in liquid nitrogen.

IHC

Mouse intestinal epithelium and tumors were processed for IHC as described previously (21).

Bioinformatics

We retrieved 585 transcriptomes of colorectal cancers (22) and used data as originally normalized. Spearman correlation was computed between *MKI67* Affymetrix chip probes and all other gene probes over all samples simultaneously or for each sample cluster (cancer subtypes as defined in the original publication) separately. When multiple probes were available, the pair giving the highest absolute correlation (sum of absolute values over all clusters when computed for each cluster separately) was retained. Correlation *P* values were obtained with a Student *t* distribution with n–2 degrees of freedom (n = number of samples), and corrected for multiple hypotheses (Benjamini–Hochberg; ref. 23). Correlations with FDR<0.05 were considered. Breast tumor transcriptomes (1098 samples) were obtained from the Broad GDAC interface (http://gdac.broadinstitute.org/) to The Cancer Genome Atlas (TCGA) data. We used normalized RNA-seq data as provided and generated clustering of tumors with the Firehose online tool, which found 7 sample classes (Supplementary Fig. S1). Correlation computations were performed as above.

Ki-67 proteomics data (11) were filtered to obtain a Ki-67 interactome by retaining all bait proteins with Mascot identification score ratios in the top 5% with respect to negative controls (empty vectors or unrelated protein, TRIM39). We further removed all proteins present in more than 5% of the CRAPome (24). A total of 181 proteins passed this selection (Supplementary Table S1).

Interaction networks of Ki-67 highly correlated genes were obtained using pairwise interactions found in STRING database v10 (25), considering only top 10% STRING scores.

Results

Variable Ki-67 levels correlate with cell-cycle gene expression

We first investigated whether Ki-67 expression *in vivo* varies in a cell-cycle–dependent manner by assessing Ki-67 staining on mouse intestinal epithelium. Cells in S-phase or G_2 were identified by injecting BrdUrd 2 hours prior to sacrifice. As expected, Ki-67 was absent in nonproliferating Paneth and goblet cells, whereas Ki-67 stained both BrdUrd-positive and negative nondifferentiated cells in the crypt (Fig. 1A). Ki-67 expression was higher in BrdUrd-positive cells (S-phase and G_2), and lowest in BrdUrd-negative cells, that are mostly G_1. Highest staining was observed in mitotic cells (Fig. 1A, yellow arrowheads).

We next asked whether Ki-67 expression was upregulated in tumors. We deleted exon 14 of one *Apc* allele in all intestinal epithelial cells using *Villin-Cre^{ERT2}*-mediated recombination. Adenoma formation then initiates through clonal growth from discrete epithelial cells that have lost the remaining *Apc* allele. Fig. 1B shows that Ki-67 levels were variable in both healthy tissue and in adenomas, similarly to proliferating cell nuclear antigen (PCNA; Fig. 1C), whose expression oscillates throughout the cell cycle. These results suggest that Ki-67 expression varies through the cell cycle in both normal tissues and in tumors.

We next looked at cell cycle exit *in vivo*. In the intestinal epithelium, actively proliferating crypt cells migrate upwards, exit the cell cycle, and differentiate before reaching villi. We compared Ki-67 IHC staining using different development times in serial sections of mouse intestinal epithelium. Using short exposures, Ki-67–positive staining can be seen only in cells within the proliferating crypt compartment, but longer exposures revealed low levels of Ki-67 in cells that have recently exited this compartment and started populating the adjacent villus base, where differentiating nonproliferating cells reside (Fig. 1D). Cells that have migrated up the villi have decreasing Ki-67 levels. Therefore, low Ki-67 levels reflect exit from the cell-cycle and terminal differentiation, but their assessment can be influenced by the staining protocol.

These results indicated that *MKI67* levels are linked to the cell cycle in mice. To see whether the same is true in humans, we investigated coregulated gene expression using COXPRESdb (26). Gene ontology (GO) analysis (27) revealed that mechanisms involved in mitosis and the G_2–M transition constituted the 16 most enriched biological processes of the 100 most correlated genes (Supplementary Fig. S2A; Supplementary Table S2).

To investigate genes coregulated with *MKI67* in human cancers, we first analyzed data from colorectal cancers, which have been extensively characterized at the molecular level (22). We assessed the proportion of cell-cycle genes among genes whose expression correlates with that of *MKI67*. Figure 2A shows that at a very high correlation coefficient (>0.6), around 80% of genes have a cell-cycle annotation. We next exploited STRING (25) to identify functional interactions. We superimposed high-confidence interactions determined from our

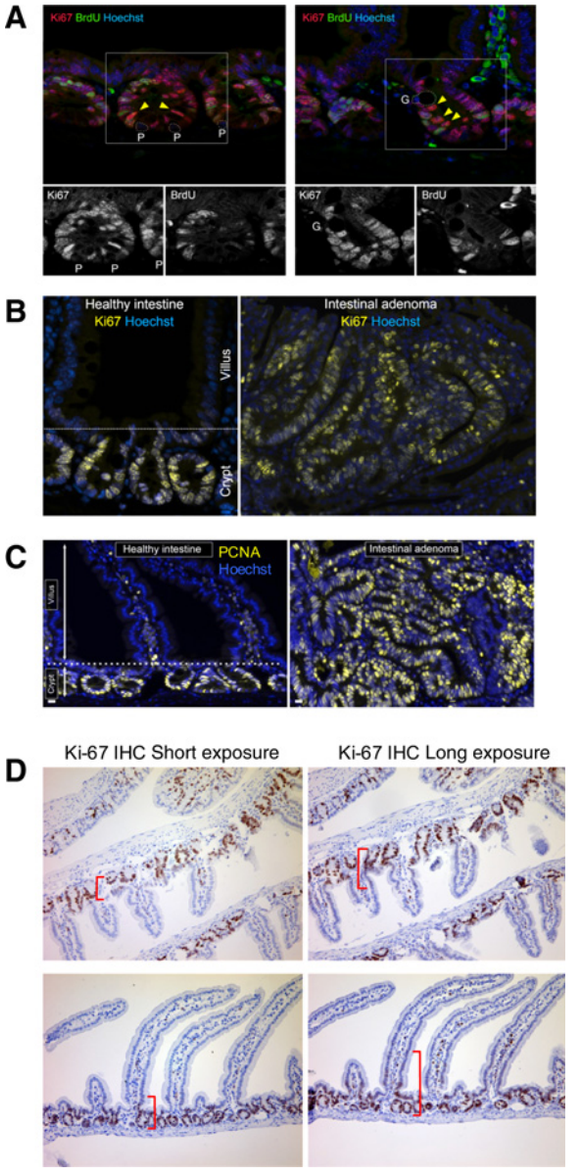

Figure 1.

Cyclic expression of Ki-67 in primary cells, cancer cells, and tumors. **A,** Cyclic Ki-67 in the mouse intestinal epithelium, as shown by immunofluorescence of Ki-67 and BrdUrd (BrdU) on paraffin-stained tissue sections from wild-type mice fixed 2 hours after BrdUrd injection. P and G, Paneth and Goblet cells, respectively. Yellow arrowheads, columnar crypt stem cells. **B,** Immunofluorescence of Ki-67 in healthy intestine and adenomas from $Apc^{-/+}$ mice showing variable levels of Ki-67 in cycling cells in the crypt and in tumors. **C,** Similar to **B**, stained for PCNA. **D,** Ki-67 IHC in serial sections of wild-type C57/BL6 mouse intestinal epithelium. Left, IHC short exposure; right, IHC saturating exposure in an adjacent section. Two examples are shown (top and bottom panels). Red brackets, visible Ki-67 labeling. Cells were counterstained by hematoxylin and eosin.

own, high-confidence Ki-67 physical interaction data (11). Figure 2B shows that many proteins encoded by these *MKI67* coregulated genes functionally interact in a cell-cycle network. Ki-67 interacts with both the mitotic and S-phase subnetworks. The remaining nodes also interact with the cell-cycle network and many have a metabolism annotation (which includes transcriptional regulation). Correlations with cell-cycle genes were maintained across colorectal cancer subtypes (Supplementary Fig. S2B). To see whether these results can be generalized to other cancers, we next interrogated TCGA with Ki-67 and searched for correlated expression across all breast cancer subtypes (28). Again, cell-cycle genes were predominant among the genes most correlated with *MKI67* (Supplementary Fig. S2C and S2D), with the top hits being cyclins (*CCNA2*, *CCNB1*, *CCNB2*), *CDK1*, *FOXM1* (a mitotic gene transcription factor; ref. 29), *BUB1B* and *DLGAP5* (which controls mitotic spindle microtubule dynamics; Fig. 2C; ref. 30).

These results indicate that the main predictor of Ki-67 mRNA levels is the cell-cycle phase, with *MKI67* most correlating with expression of genes involved in mitosis. We next experimentally analyzed Ki-67 and cyclin A2 mRNA and protein levels in a panel of human cancer cell lines: nontransformed human dermal fibroblasts (HDF) and their counterparts transformed with HPV-16 E7 oncogene, and cancer cells of different tissue origins and varying aggressiveness (U2OS, HeLa, HCT-116, MCF-7, HBL-100, CAL-51, and MDA-MB-231). As different human cancer cells express multiple smaller isoforms of Ki-67 (31), we quantified the total level of all Ki-67 species by dot-blotting. As controls, we used U2OS cells expressing nontargeting shRNA or Ki-67 shRNA (11), and HDF treated with the CDK4/CDK6 inhibitor PD0332991 (PD), which can induce senescence (32). As expected, Ki-67 shRNA or PD caused loss of both Ki-67 protein and mRNA. Ki-67 expression directly correlated with cyclin A2 expression at both protein (Fig. 2D) and mRNA (Fig. 2E) levels in all cell lines, including HDF treated with PD. Thus, Ki-67 levels are similar between cell types but depend on cell-cycle regulation.

Cell-cycle regulation of Ki-67 expression

To better understand cell-cycle variability of Ki-67 expression, we followed Ki-67 protein and mRNA levels in HDF cells synchronized throughout two cell cycles after release from quiescence. We used sequential block and release from CDK1 inhibition with RO-3306, which arrests cells at the G_2–M transition (33), and thymidine, which arrests cells in S-phase (Fig. 3A and B). Both Ki-67 and cyclin A2 mRNA levels oscillated, peaking at G_2 before decreasing in M-phase, as identified by phospho-histone H3 staining, dropping further in G_1 and rising again in the next cell cycle (Fig. 3C). Protein levels were also cyclic, peaking in mitosis (Fig. 3D). However, unlike mitotic cyclins, Ki-67 was not completely degraded during mitosis. We confirmed and extended these results to other cell lines by quantifying Ki-67 expression in asynchronous single HDF, HCT-116 or U2OS cells by immunofluorescence using markers of different cell-cycle stages (Supplementary Fig. S3A and S3B). Similar cell-cycle variation in Ki-67 expression level was found in a genome-scale proteomics and transcriptome analysis of a minimally perturbed cell cycle in human leukemic NB4 cells (34).

Next, we asked whether Ki-67 mRNA is sensitive to serum withdrawal after the restriction point, in cells released from a hydroxyurea-mediated S-phase block. Whereas D-type cyclin expression rapidly declined between S-phase and mitosis upon serum withdrawal, Ki-67 mRNA was stable, recapitulating cyclin A2 (Fig. 4A). Arresting cells in G_1 by CDK4/CDK6 inhibition with PD for 24 hours caused disappearance of Ki-67

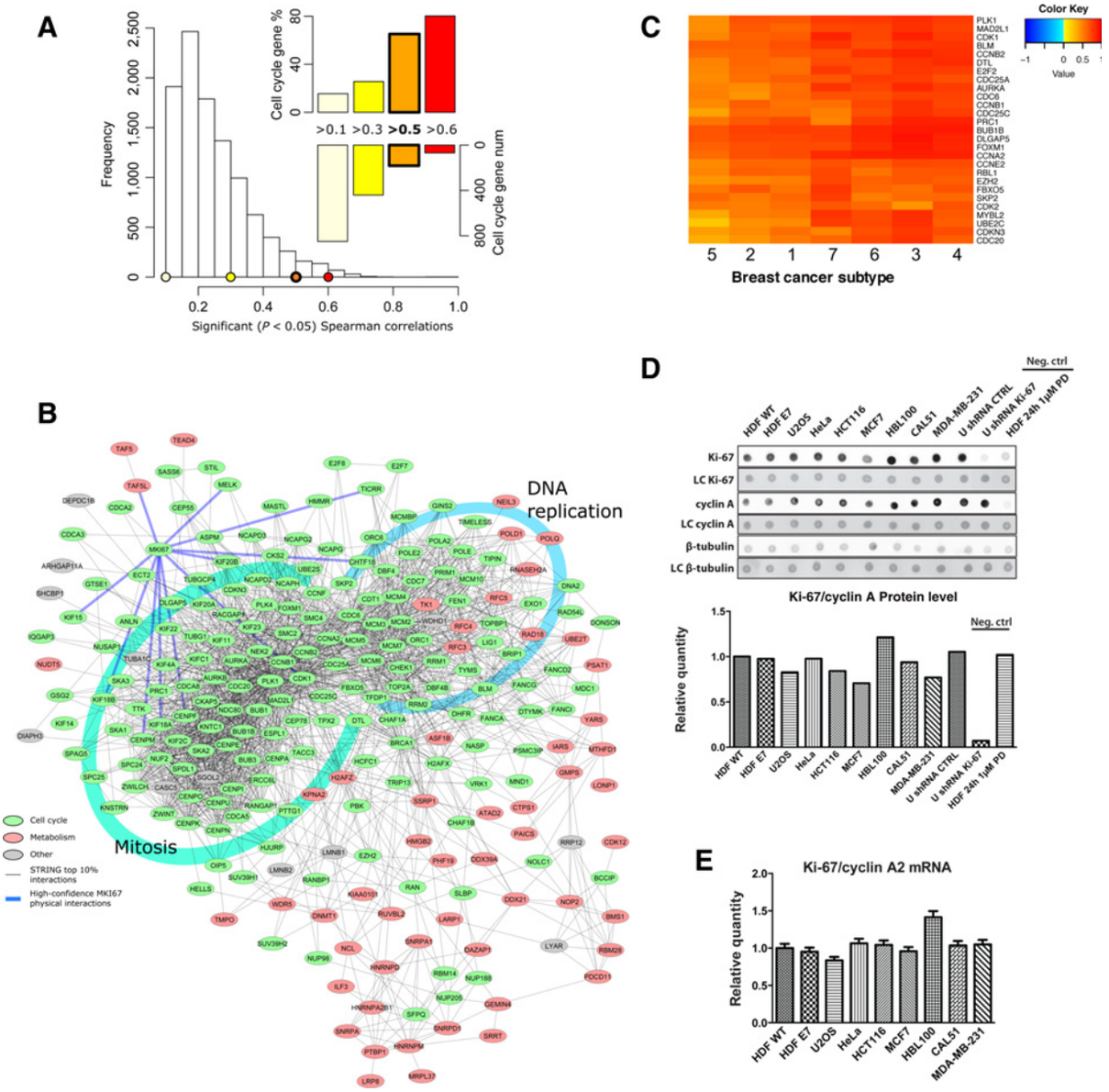

Figure 2.

Ki-67 expression is determined by the cell-cycle stage. **A,** Histogram of the number of *MKI67* significantly correlated genes in colorectal tumors with respect to Spearman correlation values (all correlations adjusted $P < 0.05$). The upper right bar plots report the proportion and number of cell-cycle genes among genes above a given correlation coefficient. **B,** Ki-67 interactome obtained combining STRING database interactions and our own Ki-67 protein physical interactions for all genes with correlation > 0.5 in **A**. **C,** Comparison between *MKI67* and other genes in TCGA breast cancer transcriptomic data showing that mitotic genes are strongly correlated with Ki-67 expression in all cancer subtypes. For a full heatmap of correlated genes with a cancer annotation see Supplementary Fig. S2D. **D,** Ki-67 levels in cycling cells are comparable between primary human fibroblasts (HDF) and cancer cells. Immunodot blot of Ki-67 and cyclin A2 proteins from asynchronous cell lysates from the indicated cell lines compared with total protein as loading control (LC) and β-tubulin. Controls include U2OS stably expressing shRNA control silencing or Ki-67 silencing vectors (where Ki-67 is absent but cyclin A2 remains) or HDF arrested by treatment with PD0332991 (both Ki-67 and cyclin A2 are absent). Bottom, quantitation of results by densitometry analysis. **E,** The ratio of Ki-67 to cyclin A2 mRNA is similar in all cell lines as quantified by qRT-PCR (experiment as in **A**).

mRNA and protein. Both Ki-67 loss and G_1 arrest were prevented by inactivating RB via expression of the HPV16 E7 oncogene (Fig. 4B–E). Ki-67 protein was degraded after release from the G_2–M block (Fig. 4F), rather than throughout the cell cycle as reported for HL60 cells (6). Ki-67 degradation at the mitosis/G_1 transition suggested that it involves the ubiquitin–proteasome system, in agreement with our previous demonstration (13) that Ki-67 downregulation is dependent on FZR1 (also known as CDH1), which activates the Anaphase-Promoting Complex (APC/C). Indeed, inhibiting the proteasome with

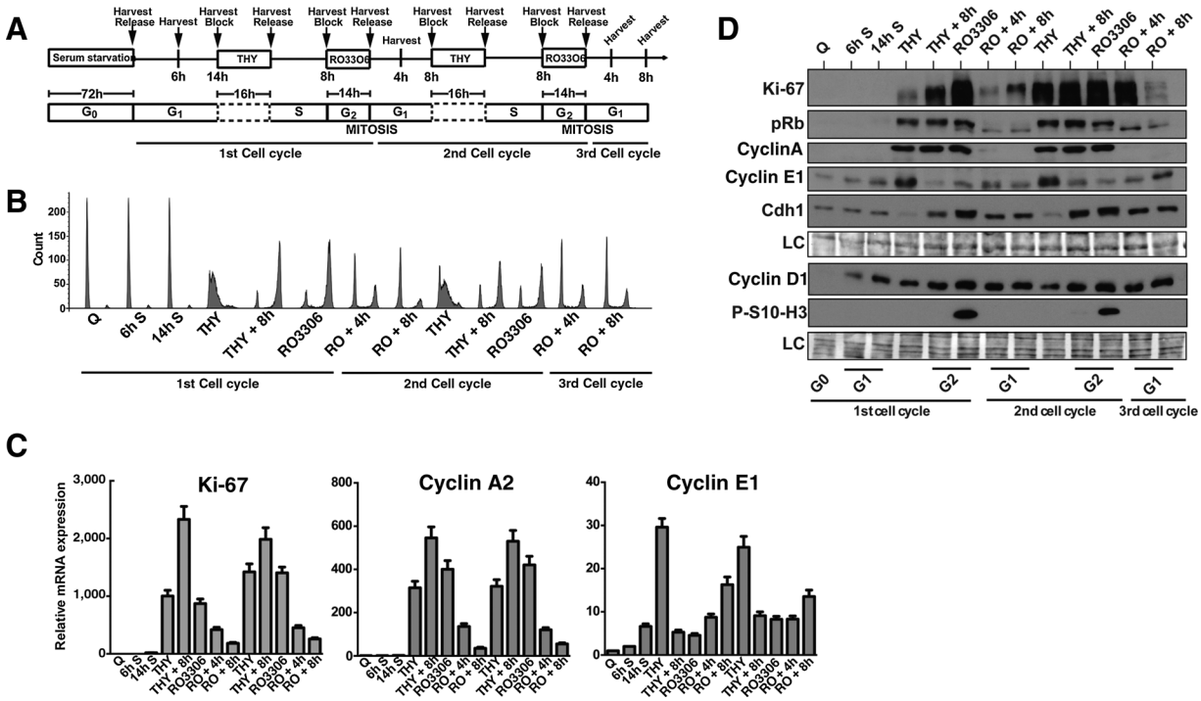

Figure 3.

Ki-67 expression is dynamically controlled by a cell-cycle–regulatory network. **A,** Scheme. HDFs were sequentially synchronized over two cell cycles upon entry from quiescence. **B,** DNA content was analyzed by flow cytometry. **C,** qRT-PCR analysis of indicated mRNA. **D,** Western blotting of indicated proteins (Q, quiescence; S, serum stimulation; THY, thymidine block; THY +, time point after release from thymidine block; RO3306, RO3306 block; RO +, time point after release from RO3306 block). LC, loading control (amido black).

MG132 prevented loss of Ki-67 protein upon PD treatment (Fig. 4G). Thus, CDK4/CDK6 inhibition eliminated Ki-67 expression by G_1 arrest, where Ki-67 mRNA expression is abolished and ubiquitin-mediated protein degradation occurs.

Ki-67 expression is a late marker of cell-cycle entry and persists on cell-cycle exit

We next investigated how Ki-67 levels change in cells entering or leaving the cell cycle. First, HDFs were released from serum starvation, and DNA content and Ki-67 expression were determined over 30 hours (Fig. 5A). Very low levels of Ki-67 were detected in serum-starved cells, although cyclin A2 was absent and no cells were in S-phase. Whereas cyclin D1 levels rose rapidly, Ki-67 protein remained at a low level throughout the G_0–G_1 transition and rose upon entry into S-phase, when cyclin A2 became detectable. The major increase in Ki-67 expression occurred between S-phase and mitosis.

To verify whether persistent Ki-67 expression is a consistent feature of physiologically quiescent cells, we analyzed human umbilical cord T lymphocytes, which enter the cell cycle upon IL2 stimulation. Ki-67 was completely undetectable in non-stimulated T-lymphocytes. Again, Ki-67 appeared at a late stage, after 48-hour stimulation, coincident with cyclin A2 expression (Fig. 5B).

We reasoned that low level Ki-67 might persist in early stages of cell-cycle arrest and is gradually eliminated. To test this, we assessed Ki-67 expression by immunofluorescence in individual cells arrested using different approaches. We induced quiescence either by contact inhibition or serum starvation, or by DNA-damaging agents, ICRF-193 or bleomycin (Supplementary Fig. S4; ref. 20). Residual nuclear Ki-67 staining could clearly be seen in quiescent cells and was higher in contact-inhibited cells, which more readily enter the cell cycle when released, than serum-starved cells (Fig. 5C and D). However, Ki-67 was similar to background staining in cells with DNA damage (Fig. 5E and F). In all cases, cyclin A2 disappearance confirmed cell-cycle exit. Background Ki-67 levels could be detected 1 day after bleomycin treatment (Fig. 5F), but were essentially undetectable after 3 days and 7 days, by which time (7 days) senescent cells were readily visualized by β-galactosidase activity staining (Supplementary Fig. S5).

Taken together, these results show that high Ki-67 expression is a late marker of cell-cycle entry and its highest levels occur in G_2 and M-phase. Quiescent cells and cells entering the cell cycle have low Ki-67, and Ki-67 is undetectable in deeply quiescent or senescent cells.

Ki-67 expression reveals responses to drugs that target cell proliferation

Our results suggest that Ki-67 expression could be useful for assessing cellular responses to CDK4/CDK6 inhibition. However, as neither CDK4/CDK6 nor Ki-67 are essential for cell proliferation in all cells, it was important to verify whether Ki-67 expression always recapitulates cell proliferation status upon CDK4/CDK6 inhibition. We tested this using a panel of cancer cell lines treated with a range of concentrations of PD for 24 hours, and then exposed to 5-ethynyl-2-deoxyuridine (EdU) for a further 24 hours, to assess DNA replication. Samples were taken to

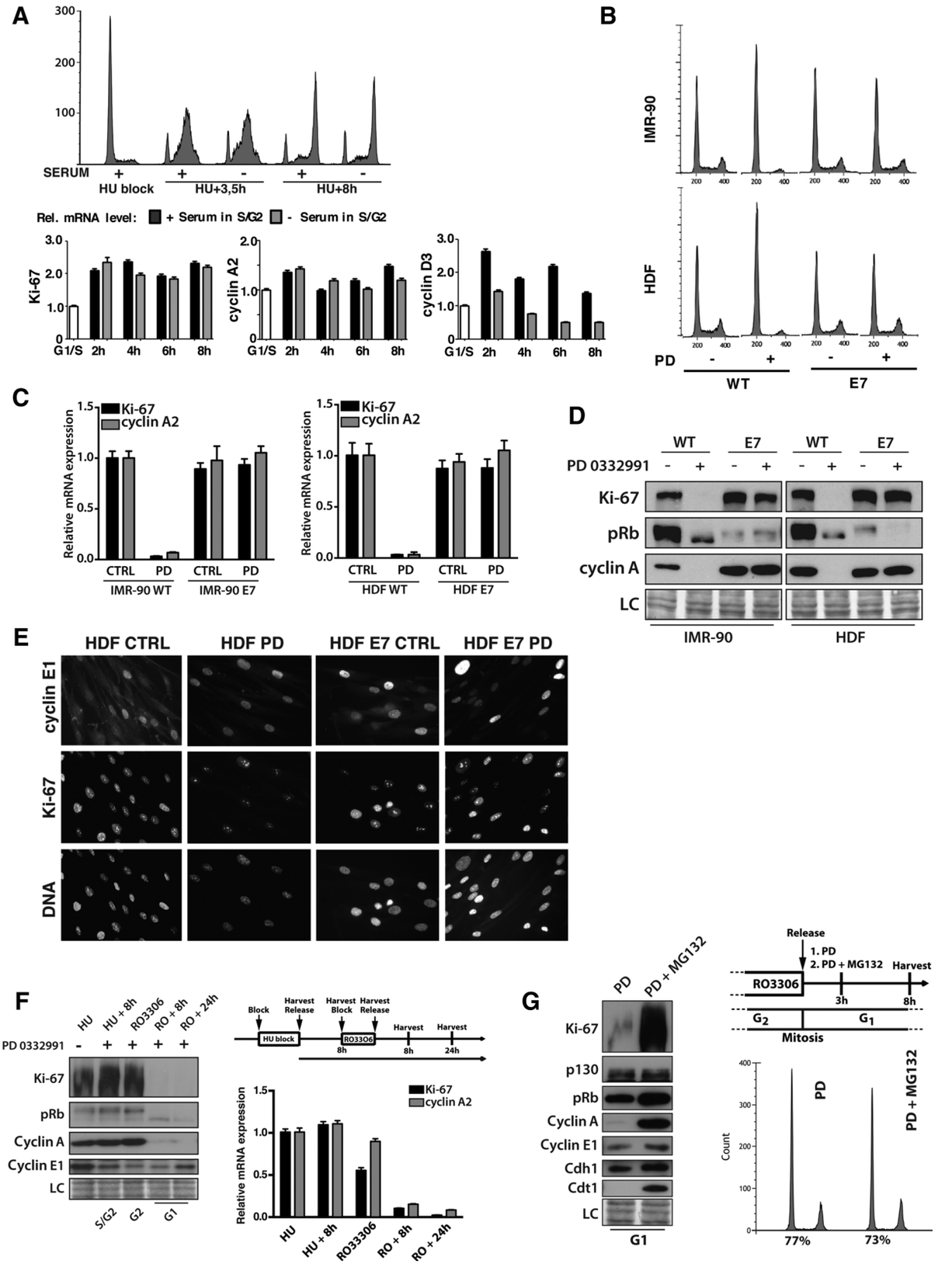

measure Ki-67 protein and mRNA. This revealed that the cell-cycle responses to PD strictly correlated with the effects on Ki-67 mRNA and protein levels (Fig. 6A). In RB-positive cells, this was further correlated with loss of RB phosphorylation. PD most effectively prevented S-phase onset and downregulated Ki-67 in RB-positive MDA-MB-231 and MCF7 cells. HCT-116 cells, which are RB-positive, responded poorly to PD, possibly because they are also mutated for *KRAS* and *PI3KCA* (35). PD had no effect on low-RB–expressing HeLa cells.

To confirm the robustness of Ki-67- and cyclin A2-correlated expression upon PD treatment, we interrogated the Cancer Cell Line Encyclopedia (36). We also compared expression of *Mki67* with mRNA encoding cyclins B1, D1, and D3. This showed an extremely tight correlation between *MKI67* and *CCNA2* (cyclin A2) in all cell lines at any concentration of PD, and a good, but slightly lower, correlation with CCNB1 (cyclin B1; Fig. 6B). Ki-67 and D-type cyclin expression was not correlated. This data also shows that PD sensitivity (inversely related to IC_{50}) and Ki-67 levels were not correlated. Thus, there is no general value of Ki-67 expression in predicting sensitivity to PD. We then extended this question to all drugs analyzed in the CCLE. Considering all drugs together, *MKI67* expression showed no correlation with drug-sensitivity (IC_{50}; Supplementary Fig. S6A). However, *MKI67* and CCNA2 showed a weak correlation with sensitivity to topoisomerase inhibitors irinotecan and topotecan (Supplementary Fig. S6B).

Finally, we performed an experiment in mice to see whether effects of CDK4/CDK6 inhibition on cell proliferation and Ki-67 expression correlate in tumors *in vivo*. We compared PD-sensitive and resistant cell lines, MDA-MB-231 and MDA-MB-468, respectively (37). We engrafted these lines subcutaneously into nude mice and allowed tumors to grow to 200 mm^3 before treating mice with vehicle or PD for 5 days by oral administration. As expected from *in vitro* experiments, PD treatment arrested tumor growth from MDA-MB-231, but not MDA-MB-468 (Fig. 7A). This was reflected by strongly decreased IHC staining for cyclin A2, PCNA, and Ki-67 in MDA-MB-231, but no change in these markers in MDA-MB-468 (Fig. 7B). The number of cells scored positive for Ki-67 and PCNA was most similar in untreated samples, and higher than cyclin A. This is because Ki-67 and PCNA, although variable, are present throughout the cell cycle, whereas cyclin A is only present from S-phase to G_2. However, responses to PD in MDA-MB-231 were more complete for Ki-67 and cyclin A than for PCNA, where low level staining remained in a minority of treated cells. This might reflect a difference in half-life of PCNA compared with cyclin A and Ki-67, both of which are degraded by the APC/C in mitosis and G_1. Analysis by qRT-PCR confirmed that protein levels were recapitulated by mRNA levels, and also showed that cyclin D mRNA levels did not change (Fig. 7C). Thus, Ki-67 is a good marker for cell proliferation status in response to PD *in vivo*.

Discussion

In light of the variability of the Ki-67 index in cancer biopsies and lack of consistent correlation with responses to therapy, it is important to understand how Ki-67 expression is controlled. We find that cell-cycle regulation accounts for variability in Ki-67 expression in primary cells and cancer cell lines as well as in tumors and human cancers. Thus, low and high level Ki-67 should be scored as positive to determine the Ki-67 labeling index. However, extremely low Ki-67 levels can be detected in quiescent cells by IHC upon long exposure. Unlike the situation in senescent cells, which have no Ki-67, such low levels of Ki-67 staining persist in cells that have recently stopped proliferating and entered quiescence.

Ostensibly, this is incompatible with the idea of Ki-67 as a specific marker for proliferating cells, but is consistent with a previous report that Ki-67 could be detected at sites of ribosomal RNA synthesis in quiescent cells (38). We speculate that a basal level of Ki-67 might be a marker for the recently described primed state for cell-cycle reentry termed G(Alert) (39). This basal level of Ki-67 in arrested cells contributes to the variability in assessments of Ki-67 staining index in cancers as cells might be variably classed as Ki-67–positive or negative. Basal Ki-67 expression might itself be a useful marker to identify cells within tumors that proliferate slowly or are quiescent, and thus are more resistant to chemotherapy or radiotherapy than proliferating cells (40). Such populations appear to be responsible for relapse after chemotherapy in colorectal cancer patients (41). Furthermore, in breast cancer, cells with low proliferation rates, and therefore low Ki-67 index, can sustain the tumor niche for highly proliferative clones, with which they remain in equilibrium (42). Quiescent cells would likely be undetectable upon standard IHC analysis, but our data suggest that they could be identified and distinguished from proliferating or senescent cells by more sensitive IHC analysis. Cells with such low levels of Ki-67 should be scored separately from cells with higher Ki-67 levels, which are proliferating, as they may have implications for prognosis of relapse.

We find that Ki-67 cell-cycle regulation relies on two opposing mechanisms dependent on conserved cell-cycle regulators: CDK4/CDK6 phosphorylates RB, allowing Ki-67 mRNA expression in G_1, and this is opposed by protein degradation in late mitosis and early G_1 by the ubiquitin–proteasome system. This

Figure 4.

Ki-67 expression is restricted to proliferating cells by CDK4/CDK6 and proteasome-mediated degradation. **A,** Top, flow cytometry DNA content profiles of HDF released for the indicated time from a HU block in the absence or presence of serum. Bottom, qRT-PCR analysis of the indicated mRNAs during this time course. **B,** Flow cytometry DNA content profiles of WT (left) or HPV-E7-expressing (right) IMR-90 (top) or HDF (bottom) treated or not with PD0332991 (PD) for 24 hours. **C,** Analysis of cyclin A2 and Ki-67 mRNA levels by qRT-PCR in the experiment from **B**. **D,** Western blot analysis of Ki-67, cyclin A2, and total RB1 protein (pRb) in the experiment from **B**. LC, loading control (amido black). **E,** Immunofluorescence of Ki-67 and cyclin E1 in HDFs, with or without HPV16-E7 oncogene expression, treated or not with PD for 24 hours. **F,** HDFs were synchronized with HU, followed by RO3306 and released to G_1 with PD0332991 for indicated times. Top right, scheme of the experiment; left, Western blot analysis of indicated proteins. LC, loading control. Bottom right, qRT-PCR analysis of Ki-67 and cyclinA2 mRNA levels. (HU, hydroxyurea block; HU +, release from HU block; RO3306, RO3306 block; RO +, release from RO3306 block). **G,** HDFs were blocked in G_2 with RO3306, released in the presence of PD0332991 (PD), with or without MG132 (added 3 hours after release from RO3306 block). Cells were collected 8 hours after release from RO3306 block and the indicated proteins were analyzed by Western blotting (left). LC, loading control. Right, FACS analysis of cell cycle distribution indicates similar number of cells in G_1.

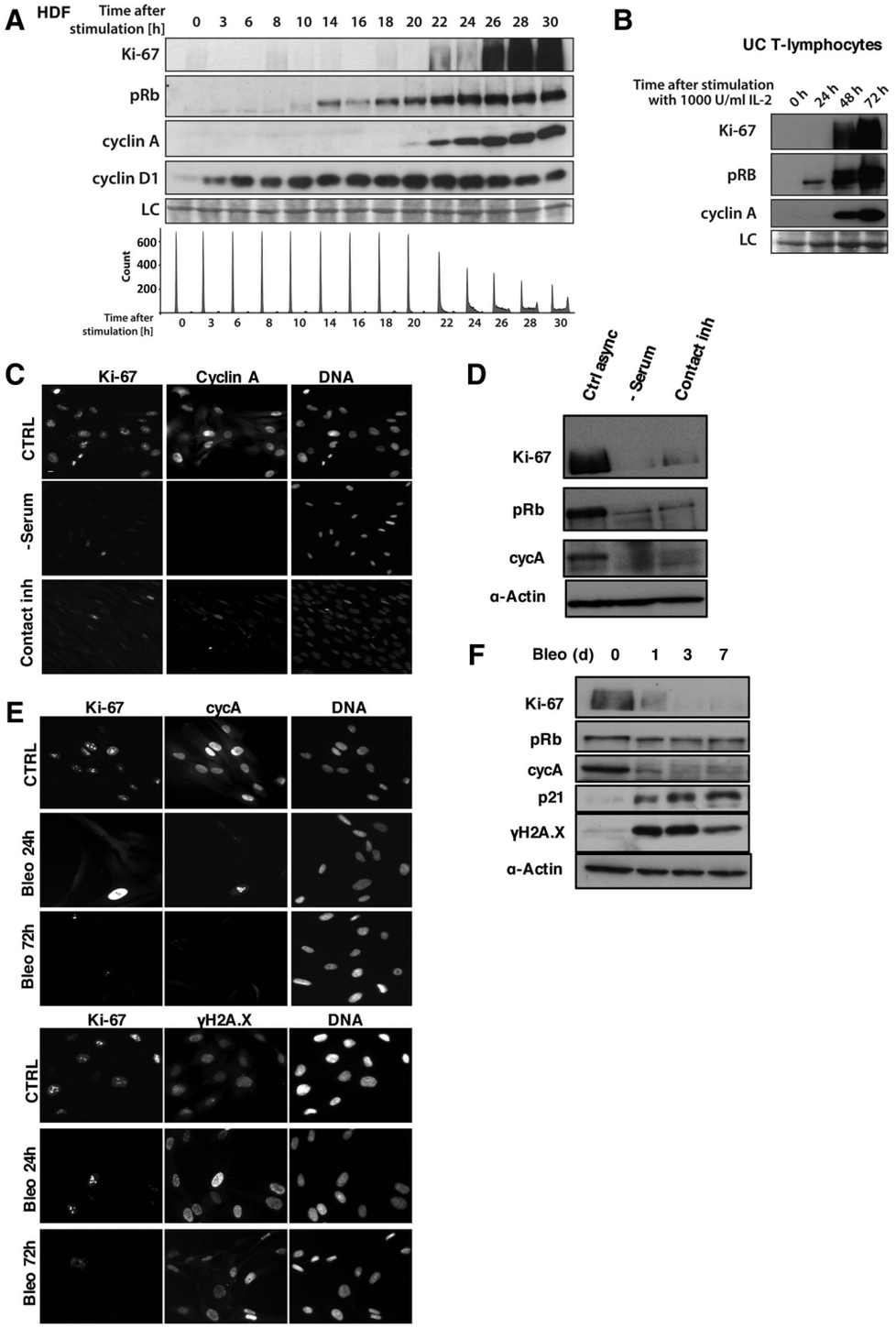

Figure 5.

Ki-67 is expressed at low levels in early cell-cycle arrest *in vitro*. **A,** Top, Western blot for indicated proteins in HDF upon cell-cycle entry and progression. LC, loading control. Bottom, DNA flow cytometry profiles. **B,** Western blot analysis of the indicated proteins in a time course of lymphocytes purified from umbilical cordon blood and stimulated by the addition of IL2 to the media. LC, loading control (amido black). **C,** Ki-67 immunofluorescence in HDFs, control or growth arrested by serum starvation (-serum) or contact inhibition (contact inh), stained for Ki-67 or cyclin A2. Scale bar, 10 μm. **D,** Ki-67, total RB (pRb), and cyclin A2 Western blot analysis upon growth arrest by serum starvation or contact inhibition. **E,** Immunofluorescence for the indicated proteins in asynchronous HDFs (CTRL) or HDFs arrested by DNA damage by 24 or 72 hours treatment with bleomycin (Bleo). **F,** Time course (days) of Ki-67 protein expression upon bleomycin treatment. The indicated proteins were analyzed by immunoblotting.

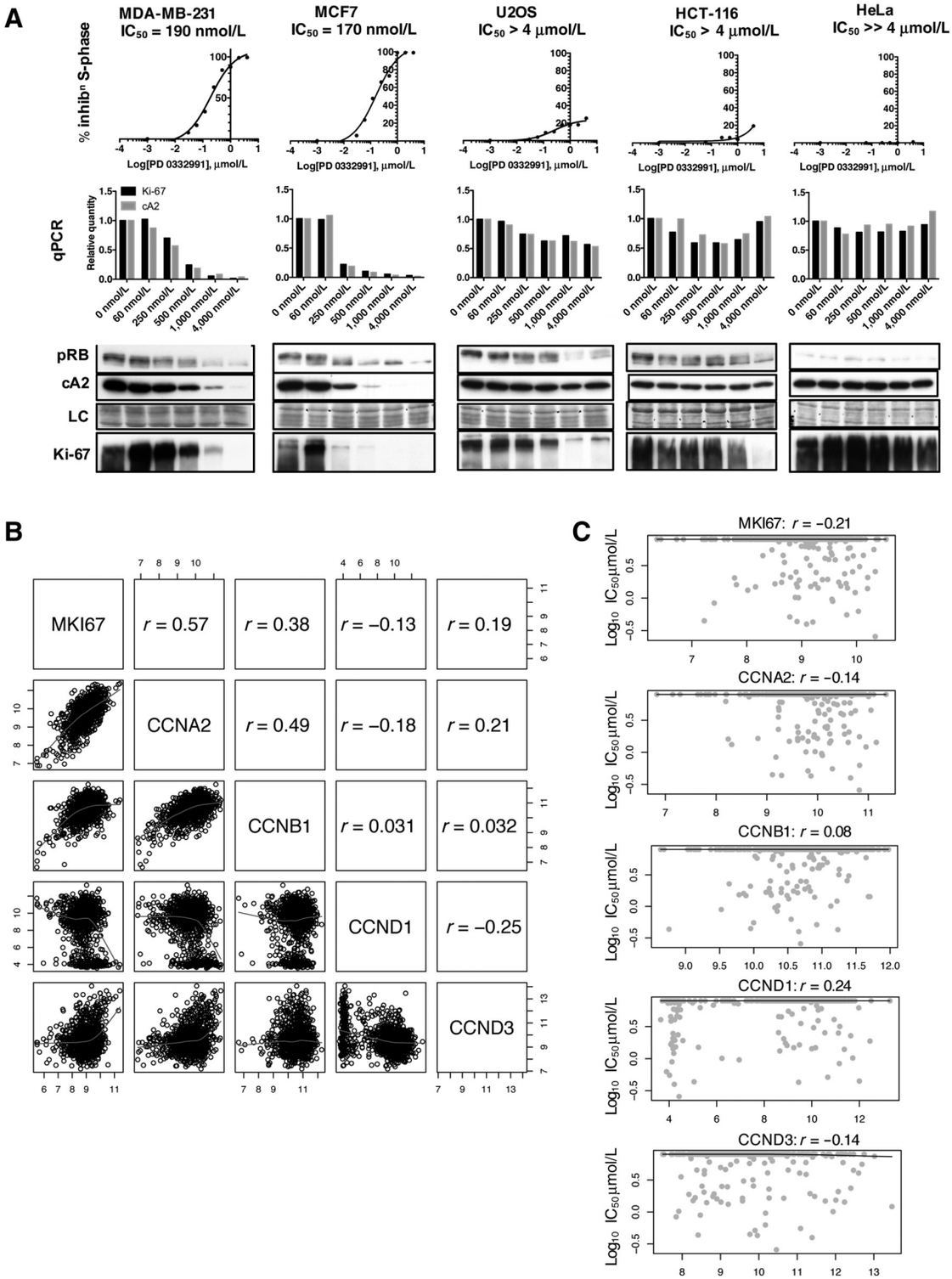

Figure 6.

Responses to CDK4/CDK6 inhibition of cancer cell lines correlate with effects on Ki-67 mRNA and protein. **A,** After treatment with the indicated dose of the PD0332991 for 24 hours, EdU was added and EdU-positive staining assessed after a further 24 hours by flow cytometry. Middle, qRT-PCR quantification of Ki-67 and cyclin A2 (cA2) mRNA. Bottom, Western blotting for total RB1 (pRb), Ki-67, and cyclin A2 (cA2), with loading controls (LC; amido black). **B,** Correlation (Spearman) between *MKI67* and *CCNA2, CCNB2, CCND1*, and *CCND3* across all CCLE cell line transcriptomes. **C,** Correlation between response to PD0332991 and *MKI67*, *CCNA2, CCNB2, CCND1*, and *CCND3* expression levels in CCLE cell lines.

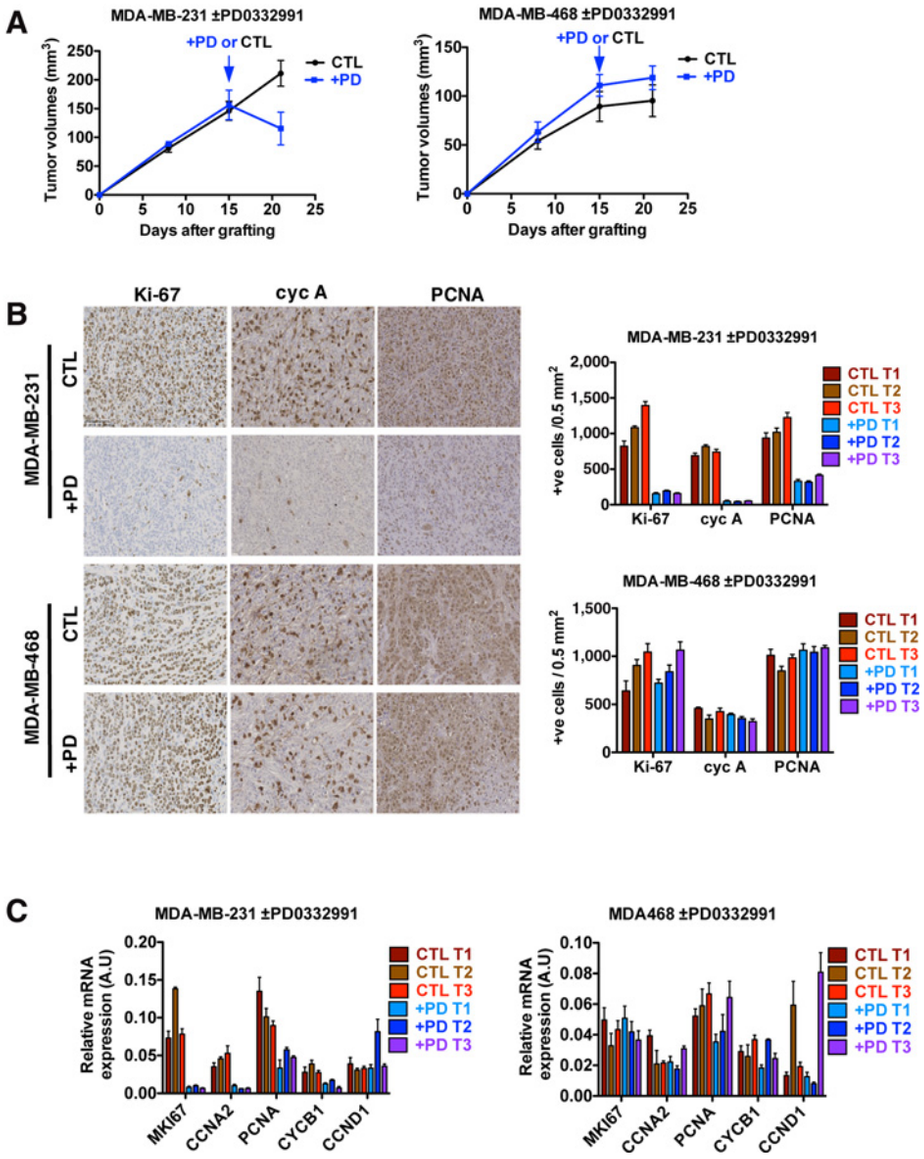

Figure 7.
Ki-67 is a good biomarker for responses to CDK4/CDK6 inhibition *in vivo*. **A,** Tumor growth in nude mice of xenografts of MDA-MB-231 cells (left) or MDA-MB-468 cells (right) treated for 5 days from day 15 with vehicle control (CTL) or PD0332991 (PD) by oral administration. Error bars, SEM (n = 3–6 mice). **B,** Left, IHC of tumors dissected after treatment and stained for the indicated proteins. Right, graphs showing scores of positive (+ve) cells per 0.5 mm^2 area for each marker; mean ± SEM (n = 3) for each of three separate tumors from different mice per cell line and treatment (T1–T3). **C,** Graphs showing relative mRNA levels for the indicated genes in tumors after treatment, as determined by qRT-PCR. Means ± SEM (n = 3), for each of three separate tumors from different mice per cell line and treatment (T1–T3).

corroborates our recent findings that Ki-67 protein expression is maintained in nonproliferating cells mutated for the *Fzr1* gene, which encodes the CDH1 activator of the mitotic/G1 ubiquitin ligase, APC/C. Eliminating both RB and APC/C-CDH1 bypasses CDK4/CDK6 inhibition in breast cancer cells, and their combined gene knockout in nematodes circumvents the requirement for CDK4 (43). Thus, CDK4/CDK6 inhibition might both prevent Ki-67 transcription and promote its degradation. The mechanisms regulating Ki-67 expression link it to the cell cycle, resulting in maximal Ki-67 levels in mitosis and minimal Ki-67 levels in late G_1. In cancer cells, inhibition of entry into S-phase strictly correlates with downregulation of Ki-67. Although tumor explants with inactivated RB, which do not respond to PD0332991, have a higher initial Ki-67 index (17), we find that in CCLE data, Ki-67 expression does not generally correlate with PD0332991 sensitivity. However, we confirmed *in vivo* that PD0332991 treatment abrogates Ki-67 expression only when it abolishes cell proliferation. This provides a rationale for using Ki-67 expression as a biomarker to measure responses to PD0332991 or other CDK4/CDK6 inhibitors currently under development. Indeed, recent phase II trials with one such inhibitor, abemaciclib, found that it significantly reduced Ki-67 expression in patients with untreated early-stage breast cancer (44). Our data confirm that this reliably indicates reduced cell proliferation.

It has long been assumed that Ki-67 is essential for cell proliferation, and several previous studies have supported this notion (45–50). However, using mice mutant for Ki-67, we recently demonstrated that, rather than controlling cell proliferation directly, Ki-67 is required to organise heterochromatin in proliferating cells (11). Nevertheless, Ki-67 downregulation using oncolytic viruses armed with Ki-67 shRNA decreased tumor growth in xenograft experiments in immunodeficient mice (50). Taken together, this suggests that even if Ki-67 is not

required for cell proliferation directly, it might promote tumorigenesis. Further analysis will be required to determine whether Ki-67 expression is required for tumorigenesis and its biochemical mechanisms of action.

Taken together, our results show that the average level of Ki-67 mRNA and protein in proliferating cells is similar and independent of cell type, and its levels in any one cell depend on the cell-cycle phase. In all circumstances examined, including CDK4/CDK6 inhibition, loss of Ki-67 reflected loss of cell proliferation. Thus, Ki-67 expression can be used as a biomarker for inhibition of cell proliferation by CDK4/CDK6 inhibitors, and probably any drug.

Disclosure of Potential Conflicts of Interest

No potential conflicts of interest were disclosed.

Authors' Contributions

Conception and design: M. Sobecki, K. Mrouj, L. Krasinska, V. Dulic, D. Fisher
Development of methodology: J. Colinge
Acquisition of data (provided animals, acquired and managed patients, provided facilities, etc.): M. Sobecki, F. Gerbe, P. Jay, V. Dulic, D. Fisher
Analysis and interpretation of data (e.g., statistical analysis, biostatistics, computational analysis): M. Sobecki, J. Colinge, F. Gerbe, P. Jay, V. Dulic, D. Fisher
Writing, review, and/or revision of the manuscript: J. Colinge, L. Krasinska, V. Dulic, D. Fisher
Administrative, technical, or material support (i.e., reporting or organizing data, constructing databases):
Study supervision:

Acknowledgments

The authors thank the members of the Fisher laboratory for helpful discussions, technical staff of MRI imaging facility and IGMM and IGF mouse facilities, IRCM Cell culture unit of Montpellier SIRIC (INCa-DGOS-Inserm 6045) for cell lines, Karim Chebli and Susan Prieto for help with xenograft experiments, and Benedicte Lemmers and Susana Prieto for help with immunohistochemistry.

Grant Support

This work was supported by grants from the GEFLUC LR, Agence Nationale de la Recherche (ANR-09-BLAN-0252) and the Ligue Nationale contre le Cancer (EL2010.LNCC/DF and EL2013.LNCC/DF; all to D. Fisher). Further funding was provided by Worldwide Cancer Research (16-0006 to D. Fisher). M. Sobecki was supported by the Ligue Nationale Contre le Cancer and by the Fondation pour la Recherche Médicale. K. Mrouj was supported by the Ligue Nationale contre le Cancer. J. Colinges was supported by the Fondation ARC pour la Recherche sur le Cancer (PJA 20141201975).

The costs of publication of this article were defrayed in part by the payment of page charges. This article must therefore be hereby marked *advertisement* in accordance with 18 U.S.C. Section 1734 solely to indicate this fact.

Received March 11, 2016; revised April 8, 2016; accepted March 2, 2017; published OnlineFirst March 10, 2017.

References

1. Cuzick J, Dowsett M, Pineda S, Wale C, Salter J, Quinn E, et al. Prognostic value of a combined estrogen receptor, progesterone receptor, Ki-67, and human epidermal growth factor receptor 2 immunohistochemical score and comparison with the Genomic Health recurrence score in early breast cancer. J Clin Oncol 2011;29:4273–8.
2. Dowsett M, Nielsen TO, A'Hern R, Bartlett J, Coombes RC, Cuzick J, et al. Assessment of Ki67 in breast cancer: recommendations from the International Ki67 in Breast Cancer working group. J Natl Cancer Inst 2011;103:1656–64.
3. Hao S, He Z-X, Yu K-D, Yang W-T, Shao Z-M. New insights into the prognostic value of Ki-67 labeling index in patients with triple-negative breast cancer. Oncotarget 2016;7:24824–31.
4. Wang W, Wu J, Zhang P, Fei X, Zong Y, Chen X, et al. Prognostic and predictive value of Ki-67 in triple-negative breast cancer. Oncotarget 2016;7:31079–87.
5. Endl E, Gerdes J. The Ki-67 protein: fascinating forms and an unknown function. Exp Cell Res 2000;257:231–7.
6. Bruno S, Darzynkiewicz Z. Cell cycle dependent expression and stability of the nuclear protein detected by Ki-67 antibody in HL-60 cells. Cell Prolif 1992;25:31–40.
7. Pei DS, Qian GW, Tian H, Mou J, Li W, Zheng JN. Analysis of human Ki-67 gene promoter and identification of the Sp1 binding sites for Ki-67 transcription. Tumour Biol 2012;33:257–66.
8. Tian H, Qian GW, Li W, Chen FF, Di JH, Zhang BF, et al. A critical role of Sp1 transcription factor in regulating the human Ki-67 gene expression. Tumour Biol 2011;32:273–83.
9. Ren B, Cam H, Takahashi Y, Volkert T, Terragni J, Young RA, et al. E2F integrates cell cycle progression with DNA repair, replication, and G(2)/M checkpoints. Genes Dev 2002;16:245–56.
10. Ishida S, Huang E, Zuzan H, Spang R, Leone G, West M, et al. Role for E2F in control of both DNA replication and mitotic functions as revealed from DNA microarray analysis. Mol Cell Biol 2001;21:4684–99.
11. Sobecki M, Mrouj K, Camasses A, Parisis N, Nicolas E, Llères D, et al. The cell proliferation antigen Ki-67 organises heterochromatin. eLife 2016;5:e13722.
12. Cuylen S, Blaukopf C, Politi AZ, Müller-Reichert T, Neumann B, Poser I, et al. Ki-67 acts as a biological surfactant to disperse mitotic chromosomes. Nature 2016;535:308–12.
13. Cidado J, Wong HY, Rosen DM, Cimino-Mathews A, Garay JP, Fessler AG, et al. Ki-67 is required for maintenance of cancer stem cells but not cell proliferation. Oncotarget 2016;7:6281–93.
14. Malumbres M, Sotillo R, Santamaria D, Galan J, Cerezo A, Ortega S, et al. Mammalian cells cycle without the D-Type cyclin-dependent kinases Cdk4 and Cdk6. Cell 2004;118:493–504.
15. Choi YJ, Li X, Hydbring P, Sanda T, Stefano J, Christie AL, et al. The requirement for cyclin D function in tumor maintenance. Cancer Cell 2012;22:438–51.
16. Finn RS, Crown JP, Lang I, Boer K, Bondarenko IM, Kulyk SO, et al. The cyclin-dependent kinase 4/6 inhibitor palbociclib in combination with letrozole versus letrozole alone as first-line treatment of oestrogen receptor-positive, HER2-negative, advanced breast cancer (PALOMA-1/TRIO-18): a randomised phase 2 study. Lancet Oncol 2015;16:25–35.
17. Dean JL, McClendon AK, Hickey TE, Butler LM, Tilley WD, Witkiewicz AK, et al. Therapeutic response to CDK4/6 inhibition in breast cancer defined by ex vivo analyses of human tumors. Cell Cycle 2012;11:2756–61.
18. Colnot S, Niwa-Kawakita M, Hamard G, Godard C, Le Plenier S, Houbron C, et al. Colorectal cancers in a new mouse model of familial adenomatous polyposis: influence of genetic and environmental modifiers. Lab Investig 2004;84:1619–30.
19. el Marjou F, Janssen KP, Chang BH, Li M, Hindie V, Chan L, et al. Tissue-specific and inducible Cre-mediated recombination in the gut epithelium. Genesis 2004;39:186–93.
20. Baus F, Gire V, Fisher D, Piette J, Dulic V. Permanent cell cycle exit in G2 phase after DNA damage in normal human fibroblasts. EMBO J 2003;22:3992–4002.
21. Gerbe F, van Es JH, Makrini L, Brulin B, Mellitzer G, Robine S, et al. Distinct ATOH1 and Neurog3 requirements define tuft cells as a new secretory cell type in the intestinal epithelium. J Cell Biol 2011;192:767–80.
22. Marisa L, de Reyniès A, Duval A, Selves J, Gaub MP, Vescovo L, et al. Gene expression classification of colon cancer into molecular subtypes: characterization, validation, and prognostic value. PLoS Med 2013;10:e1001453.
23. Benjamini Y, Hochberg Y. Controlling the false discovery rate: a practical and powerful approach to multiple testing. J R Stat Soc Ser B Methodol 1995;57:289–300.

24. Mellacheruvu D, Wright Z, Couzens AL, Lambert J-P, St-Denis NA, Li T, et al. The CRAPome: a contaminant repository for affinity purification-mass spectrometry data. Nat Methods 2013;10:730–6.
25. Szklarczyk D, Franceschini A, Wyder S, Forslund K, Heller D, Huerta-Cepas J, et al. STRING v10: protein-protein interaction networks, integrated over the tree of life. Nucleic Acids Res 2015;43:D447–452.
26. Okamura Y, Aoki Y, Obayashi T, Tadaka S, Ito S, Narise T, et al. COXPRESdb in 2015: coexpression database for animal species by DNA-microarray and RNAseq-based expression data with multiple quality assessment systems. Nucleic Acids Res 2015;43:D82–86.
27. Huang da W, Sherman BT, Lempicki RA. Systematic and integrative analysis of large gene lists using DAVID bioinformatics resources. Nat Protoc 2009;4:44–57.
28. The Cancer Genome Atlas Network. Comprehensive molecular portraits of human breast tumours. Nature 2012;490:61–70.
29. Fu Z, Malureanu L, Huang J, Wang W, Li H, van Deursen JM, et al. Plk1-dependent phosphorylation of FoxM1 regulates a transcriptional programme required for mitotic progression. Nat Cell Biol 2008;10:1076–82.
30. Wong J, Fang G. HURP controls spindle dynamics to promote proper interkinetochore tension and efficient kinetochore capture. J Cell Biol 2006;173:879–91.
31. Schmidt MHH, Broll R, Bruch H-P, Finniss S, Bögler O, Duchrow M. Proliferation marker pKi-67 occurs in different isoforms with various cellular effects. J Cell Biochem 2004;91:1280–92.
32. Leontieva OV, Blagosklonny MV. CDK4/6-inhibiting drug substitutes for p21 and p16 in senescence: duration of cell cycle arrest and MTOR activity determine geroconversion. Cell Cycle 2013;12:3063–9.
33. Vassilev LT.Cell cycle synchronization at the G2/M phase border by reversible inhibition of CDK1. Cell Cycle 2006;5:2555–6.
34. Ly T, Ahmad Y, Shlien A, Soroka D, Mills A, Emanuele MJ, et al. A proteomic chronology of gene expression through the cell cycle in human myeloid leukemia cells. eLife 2014;3:e01630.
35. Ahmed D, Eide PW, Eilertsen IA, Danielsen SA, Eknæs M, Hektoen M, et al. Epigenetic and genetic features of 24 colon cancer cell lines. Oncogenesis 2013;2:e71.
36. Barretina J, Caponigro G, Stransky N, Venkatesan K, Margolin AA, Kim S, et al. The cancer cell line encyclopedia enables predictive modelling of anticancer drug sensitivity. Nature 2012;483:603–7.
37. Finn RS, Dering J, Conklin D, Kalous O, Cohen DJ, Desai AJ, et al. PD 0332991, a selective cyclin D kinase 4/6 inhibitor, preferentially inhibits proliferation of luminal estrogen receptor-positive human breast cancer cell lines in vitro. Breast Cancer Res 2009;11:R77.
38. Bullwinkel J, Baron-Luhr B, Ludemann A, Wohlenberg C, Gerdes J, Scholzen T. Ki-67 protein is associated with ribosomal RNA transcription in quiescent and proliferating cells. J Cell Physiol 2006;206:624–35.
39. Rodgers JT, King KY, Brett JO, Cromie MJ, Charville GW, Maguire KK, et al. mTORC1 controls the adaptive transition of quiescent stem cells from G0 to G(Alert). Nature 2014;510:393–6.
40. Lord CJ, Ashworth A. The DNA damage response and cancer therapy. Nature 2012;481:287–94.
41. Kreso A, O'Brien CA, van Galen P, Gan OI, Notta F, Brown AM, et al. Variable clonal repopulation dynamics influence chemotherapy response in colorectal cancer. Science 2013;339:543–8.
42. Marusyk A, Tabassum DP, Altrock PM, Almendro V, Michor F, Polyak K. Non-cell-autonomous driving of tumour growth supports sub-clonal heterogeneity. Nature 2014;514:54–8.
43. The I, Ruijtenberg S, Bouchet BP, Cristobal A, Prinsen MBW, van Mourik T, et al. Rb and FZR1/Cdh1 determine CDK4/6-cyclin D requirement in C. elegans and human cancer cells. Nat Commun 2015;6:5906.
44. Hurvitz S, Abad MF, Rostorfer R, Chan D, Egle D, Huang C-S, et al. Interim results from neoMONARCH: A neoadjuvant phase II study of abemaciclib in postmenopausal women with HR + /HER2- breast cancer (BC). Ann Oncol 2016;27: LBA13.
45. Schluter C, Duchrow M, Wohlenberg C, Becker MH, Key G, Flad HD, et al. The cell proliferation-associated antigen of antibody Ki-67: a very large, ubiquitous nuclear protein with numerous repeated elements, representing a new kind of cell cycle-maintaining proteins. J Cell Biol 1993;123:513–22.
46. Kausch I, Lingnau A, Endl E, Sellmann K, Deinert I, Ratliff TL, et al. Antisense treatment against Ki-67 mRNA inhibits proliferation and tumor growth in vitro and in vivo. Int J Cancer 2003;105:710–6.
47. Starborg M, Gell K, Brundell E, Hoog C. The murine Ki-67 cell proliferation antigen accumulates in the nucleolar and heterochromatic regions of interphase cells and at the periphery of the mitotic chromosomes in a process essential for cell cycle progression. J Cell Sci 1996;109:143–53.
48. Rahmanzadeh R, Huttmann G, Gerdes J, Scholzen T. Chromophore-assisted light inactivation of pKi-67 leads to inhibition of ribosomal RNA synthesis. Cell Prolif 2007;40:422–30.
49. Zheng JN, Ma TX, Cao JY, Sun XQ, Chen JC, Li W, et al. Knockdown of Ki-67 by small interfering RNA leads to inhibition of proliferation and induction of apoptosis in human renal carcinoma cells. Life Sci 2006;78:724–9.
50. Zheng JN, Pei DS, Mao LJ, Liu XY, Mei DD, Zhang BF, et al. Inhibition of renal cancer cell growth in vitro and in vivo with oncolytic adenovirus armed short hairpin RNA targeting Ki-67 encoding mRNA. Cancer Gene Ther 2009;16:20–32.